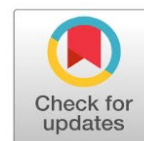




Original Research Article

Removal of colored pollutants from aqueous solutions with a poly Schiff-base based on melamine-modified MWCNT



Somayeh Farajzadeh, Peyman Najafi Moghadam*, Jabbar Khalafy

Department of Organic Chemistry, Faculty of Chemistry, Urmia University, Urmia, Iran

ARTICLE INFORMATION

Received: 31 July 2019

Received in revised: 26 September 2019

Accepted: 29 September 2019

Available online: 2 January 2020

DOI: [10.22034/ajgc.2020.100567](https://doi.org/10.22034/ajgc.2020.100567)

KEYWORDS

MWCNT

Melamine

Schiff-base

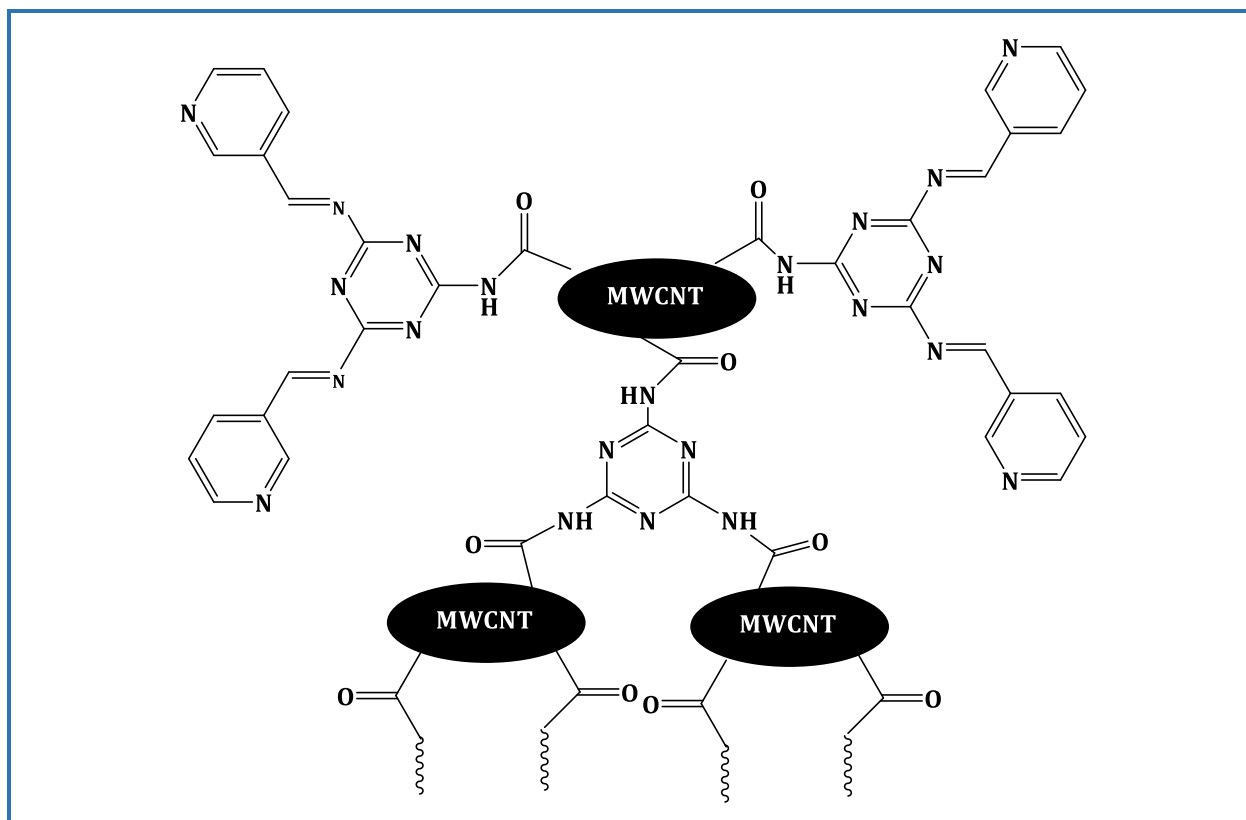
Congo red

Dye removal

ABSTRACT

Carbon nanotubes (CNTs) have been extensively explored for adsorption applications due to their well-defined cylindrical hollow structure, large surface area, high aspect ratios, hydrophobic wall, and easily modified surfaces. In the present work, a poly Schiff-base was synthesized with capability to remove the dye pollutant from aqueous solutions. For this propose, firstly, multi-walled carbon nanotube (MWCNT) was modified with melamine, then the melamine-modified MWCNT was further reacted with 3-pyridinecarboxaldehyde to synthesize the final poly Schiff-base. The prepared adsorbent was employed to assess the removal of the dye pollutants from aqueous solutions and Congo red (CR) was selected as typical dye. Different adsorption parameters such as pH, adsorbent amount, initial concentration of the dye, and contact time were investigated and optimized. By adjusting these parameters, the adsorption percentage reached to the value of 92%. Moreover, the adsorption isotherms were studied and fitted with the Langmuir, Freundlich, and Dubinin-Radushkevich (D-R) models. The kinetic studies were carried out by using the Lagergren pseudo-first-order and the Ho pseudo-second-order equations. The adsorbent was also characterized by FT-IR, TGA, and SEM techniques.

© 2020 by SPC (Sami Publishing Company), Asian Journal of Green Chemistry, Reproduction is permitted for noncommercial purposes.

Graphical Abstract**Introduction**

Nowadays, by increasing the industrial activities, contamination of water resources is a serious environmental problem and a threat to an aquatic life and food web [1–4]. The main sources of water contamination are colored by organic effluents that are produced in the industries such as textiles, rubber, paper, plastic, cosmetics, and dyes. The presence of these dyes in wastewaters, even in a small amount, is highly visible. Due to the tenacity nature, they might change the color of water, interfere with sunlight penetration, retard photosynthesis, and interfere with gas solubility in water bodies [5, 6]. Dyes with a synthetic origin and a complex aromatic molecular structure resist against light, washing, and microbial invasions with a high chemical stability [7]. Allergic dermatitis, skin irritation, carcinogenic, and mutagenic for aquatic organisms are the problems that associate with the dyes in the human health and marine organisms [8].

Congo red (CR) (sodium salt of the benzidinediazobis-1-naphthylamine-4-sulfonic acid) is one of the anionic toxic dyes. This diazo dye simply metabolizes to benzidine and its exposure causes an allergic reaction. The CR enters to various ecosystems, affecting the aquatic life and food web. It also may lead to health hazards such as difficulties in breathing, vomiting, diarrhea, and nausea [9].

Therefore, simple and efficient elimination of this compound from wastewaters before discharging to aqueous bodies is necessary. There are many treatment methods to remove the dyes from water. These methods are based on their physical, chemical, electrical, thermal, and biological properties [10]. They include coagulation [11], precipitation [12, 13], ion exchange [14, 15], physical adsorption [16, 17], membrane filtration [18, 19], electrochemical techniques [20, 21], and bioremoval [22, 23]. Among these techniques, the adsorption method has been widely used due to its high efficiency, easy operation, handling, and low cost [24–26]. The adsorbents with high capacity, high adsorption rate, and nontoxic nature are the best choice to remove the dye molecules. Active carbon has been used previously for the fast adsorption of dye contamination from wastewater [27]. However, the use of active carbon is limited due to its high cost and low regeneration [28, 29]. Recently, various materials such as activated carbon, clays and synthetic polymers including, conducting polymers, nanogel, and superparamagnetic nanocomposite are used to eliminate dyes and heavy metal ions from the wastewaters. Among the conducting polymers based adsorbents, polyaniline (PANI) and its derivatives have received significant attention due to their good adsorption capability, so they are used as adsorbents for the removal of heavy metal ions and dyes from aqueous solutions [30–32]. In the last decade, multi-walled carbon nanotube (MWCNT) has attracted a great deal of attention due to its superior properties such as large specific surface area, small size, hollow and layered structure, high efficiency, and high adsorption capacity to remove different pollutants from wastewater [33–35].

In this study, the MWCNT was modified with melamine and used as a precursor to prepare a poly Schiff-base by reacting with 3-pyridinecarboxaldehyde. Then, the prepared poly Schiff-base was used as the adsorbent for the dye pollutant from aqueous solutions. The CR was selected as a typical dye to show the ability of synthesized poly Schiff-base in adsorption of dye from aqueous solution. Moreover, different adsorption parameters were investigated and optimized. Finally, the adsorption isotherms and kinetic studies were carried out to investigate the type and mechanism of the adsorption.

Experimental

Materials and methods

Carboxylated multi-walled carbon nanotube (MWCNT) (>95%, OD=10-20 nm, ID=5-10 nm, length~30 μm) was purchased from nanocarbon Co. and used as received. 3-Pyridinecarboxaldehyde ($\geq 97.0\%$, Merck) and thionyl chloride (SOCl_2) (99%, Sigma-Aldrich) were also used without further treatment. CR dye ($\text{C}_{32}\text{H}_{22}\text{N}_6\text{Na}_2\text{O}_6\text{S}_2$, MW=696.97, $\lambda_{\text{max}}=498$ nm) was supplied by S.D. Fine chemicals,

Mumbai, and India and it was utilized without any further purifications. The chemical structure of the dye is illustrated in Figure 1.

The FT-IR and UV-vis. spectra were recorded by thermo Nicolet NEXUS 670 FT-IR Fourier transform infrared spectrophotometer (Thermo scientific, USA) and agilent 8453 diode array UV-vis. spectrophotometer (agilent technologies, USA), respectively. The thermogravimetric analysis (TGA) was studied by STA PT1000 TG-DSC (STA simultaneous thermal analysis) STA (TG-DSC/DTA) thermogravimetric analyzer (linseis thermal analysis, Germany) at a heating rate of 10 °C/min under N₂ atmosphere. The scanning electron microscopy (SEM) images were obtained from LEO 1430 VP (leo electron microscopy Ltd, UK).

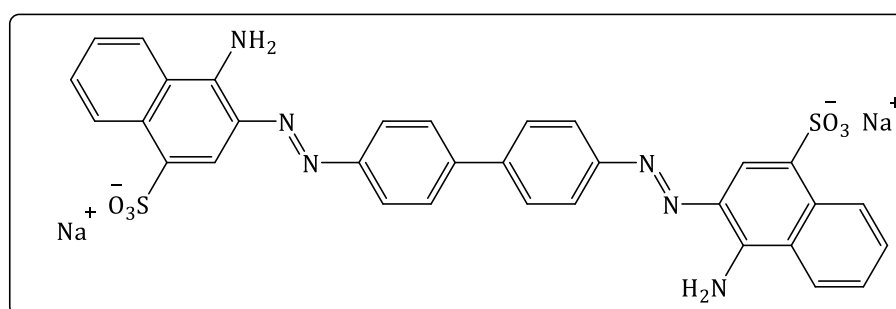


Figure 1. The chemical structure of Congo red dye

Chlorination of MWCNT

MWCNT (0.5 g) and SOCl₂ (30 mL) were also mixed and refluxed in a 100 mL round-bottom flask equipped with a condenser and a magnetic stirrer bar for 24 h under argon inert atmosphere. After that, the reaction mixture was cooled down to room temperature and the product was separated by a centrifuge (4000 rpm, 10 min), washed with dichloromethane, and dried under inert atmosphere.

Preparation of melamine-modified MWCNT (Mel-MWCNT)

The previously synthesized chlorinated MWCNT (300 mg) was dispersed in *N,N'*-dimethylacetamide (DMA) (50 mL) and an excess amount of melamine (700 mg) was added. Then triethylamine (10 mL) was added to the mixture and heated up to 110 °C for 24 h under inert atmosphere. Then, the stirrer was turned off and the product was allowed to be settled down without cooling the mixture. The supernatant was extracted from the flask, and hot water was added to it for several times and stirred to remove unreacted melamine. Finally, the product was separated by the centrifuge (4000 rpm, 20 min) and dried at room temperature.

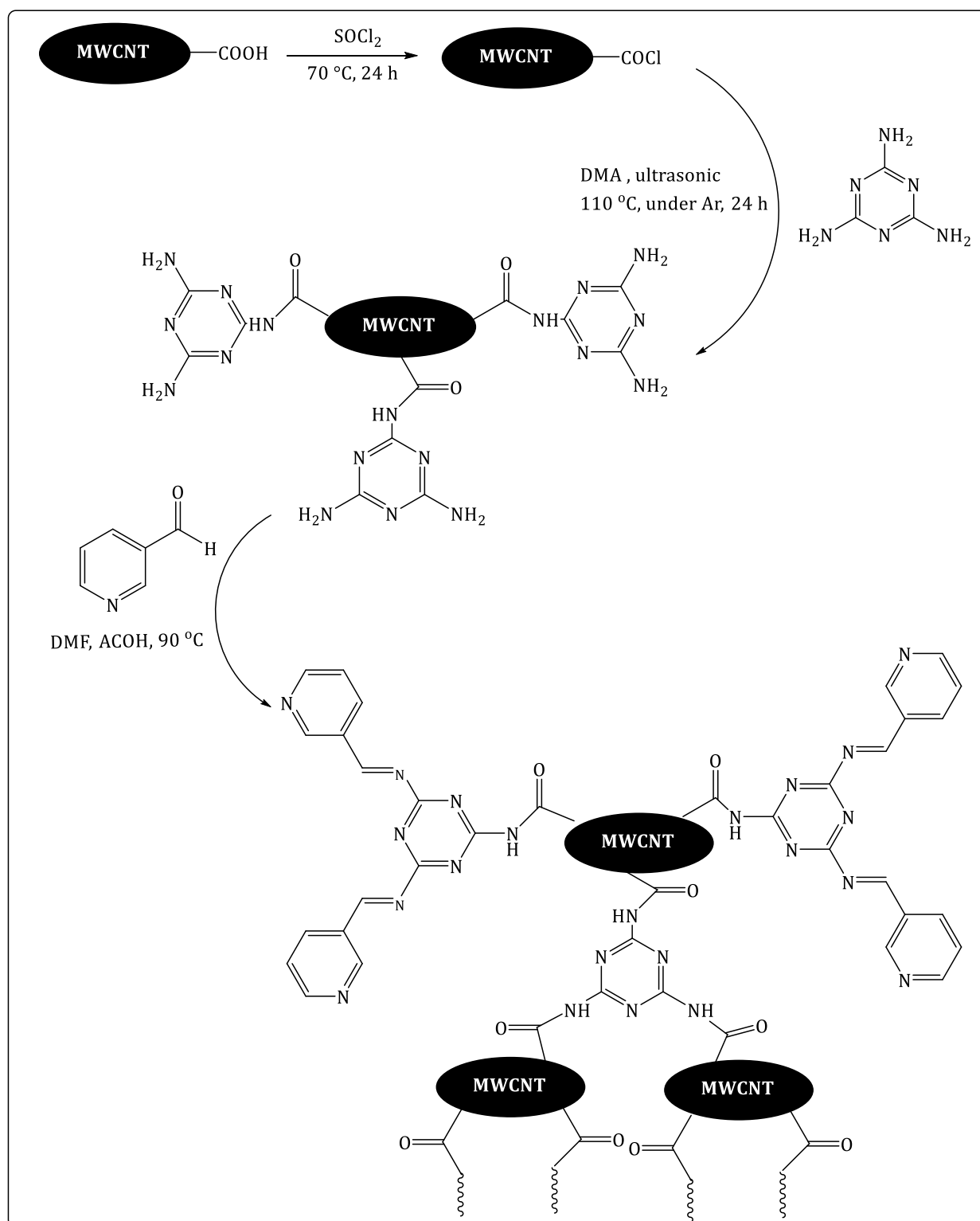
Synthesis of poly Schiff-base adsorbent

The Mel-MWCNT (100 mg) and 3-pyridinecarboxaldehyde (0.18 mL, 200 mg) were added to the DMF (10 mL) in a round-bottom flask in order to synthesize the adsorbent and then it followed by adding 3-4 drops of the glacial acetic acid. The mixture was heated up to 90 °C for 24 h. After cooling down to room temperature, we separated the final product by the centrifuge (4000 rpm, 10 min), washed it several times with methanol, and finally dried it at room temperature. The overall synthesis process is depicted in [Scheme 1](#).

To study the adsorption process at room temperature, firstly, we plotted the calibration curves for the CR dye at different pH values and the corresponding trendline equations were obtained. Then, the adsorption parameters were investigated in various pH, adsorbent amount, initial concentration of the dye, and contact time, respectively. For the optimization of the pH, 8 vials containing the dye solution (10 ppm, 20 mL) and the adsorbent (10 mg) were employed and the pH range was adjusted from 3 to 10. The vials were shaken for 1 h at 140 rpm. After separating the adsorbent by the centrifuge (4000 rpm, 10 min), we analyzed the supernatants by UV-vis. spectrophotometer. According to the results, the optimized pH value which was obtained was 5. In the next step, the adsorbent amount was optimized by employing 6 vials containing the dye solution (10 ppm, 20 mL) and different amounts of the adsorbent (2, 5, 10, 15, 20, and 30 mg). The all pH values were set at 5 and the vials were shaken for 1 h at 140 rpm. The supernatants were analyzed as described above. The optimized adsorbent amount was 15 mg. In order to optimize the initial concentration of the dye, we prepared 6 different concentrations (2, 5, 10, 15, 20, and 30 ppm). 20 mL of each solution was added to separate vials and 15 mg of the adsorbent was also added and followed by adjusting the pH at 5. Likewise previous steps, the vials were shaken for 1 h at 140 rpm and the supernatants were analyzed. The optimized initial concentration which was obtained was 10 ppm. In the final step, the contact time was optimized. A vial containing the optimized initial concentration of the dye (10 ppm, 20 mL), the optimized amount of the adsorbent (15 mg), and the optimized pH value (5) was placed on the shaker (140 rpm) and at different time intervals (5, 10, 20, 30, 45, 60, and 90 min) the supernatant was analyzed. The optimized contact time was 45 min. The obtained results are discussed in the next section. Moreover, the isothermal and kinetic studies are described subsequently.

Results and Discussion

The poly Schiff-base adsorbent was prepared by the reaction of Mel-MWCNT with 3-pyridinecarboxaldehyde. For this purpose, firstly the carboxylated MWCNT was chlorinated. The carboxylic acid functional groups were converted to the highly active acyl chlorides by the reaction with thionyl chloride. In this case, melamine could easily react and graft on the MWCNT backbone



Scheme 1. The overall synthesis route of the poly Schiff-base

(Scheme 1.). Using excess amount of melamine, the product generated free pendant NH_2 groups which was ready to react with the aldehyde in the final step. The reaction of these free NH_2 groups with the aldehyde and generation of imines led to the preparation of the poly Schiff-base adsorbent. The adsorbent had plenty of free electron pair-containing functional groups to interact with the dye.

Structural characterization

FT-IR analysis

Figure 2 depicts the FT-IR spectra of the a) MWCNT, b) chlorinated MWCNT, c) Mel-MWCNT, and d) poly Schiff-base, respectively. As can be seen in the spectrum a, the presence of the carboxylate groups is proved by the sharp peak at 1610 cm^{-1} . After chlorination, the stretching vibrations of the acyl halide carbonyl groups shifted to 1641 cm^{-1} . The reaction of the melamine with these acyl chloride groups led to the generation of the amides. In the spectrum c, the stretching vibrations of the carbonyl groups shifted to a lower wavenumber (1630 cm^{-1}) which is due to the presence of the amide groups. Unfortunately, due to overlapping, the stretching vibrations of the free pendant NH_2 groups are not shown in this spectrum but the spectrum d proves the successful preparation of the poly Schiff-base by showing the sharp imine ($-\text{CH}=\text{N}-$) stretching vibrations at 1661 cm^{-1} . The formation of imine groups is a strict reason for the presence of the free pendant NH_2 groups in the previous step.

TGA analysis

To assess the thermal stability of the samples, TGA analysis was carried out. The thermograms are depicted in Figure 3. In Figure 3a which is related to the pure carboxylated MWCNT, there is a weight loss in the beginning of the diagram which is related to the moisture of the sample. After that, the sample started losing weight from $150\text{ }^\circ\text{C}$, which is attributed to the decarboxylation of the carboxylic acid groups. In the thermogram b which is related to the final adsorbent, four degradation steps are observable. The first one is due to the moisture of the sample. After that, a rather continuous degradation started at $150\text{ }^\circ\text{C}$. Firstly, the pendant groups on the adsorbent backbone such as $-\text{COOH}$, $-\text{NH}_2$, and $-\text{CH}=\text{N}-$ start to degrade and generate CO , CO_2 , and NH_3 . The C-C bonds related to the modifying agents disjunct from the backbone depending on the type and the thermal stability of the moieties.

SEM analysis

Figure 4 demonstrates the SEM micrographs of the MWCNT (a, c) and the final poly Schiff-base (b, d) in two different magnifications. The change in the morphology of the modified sample and pure

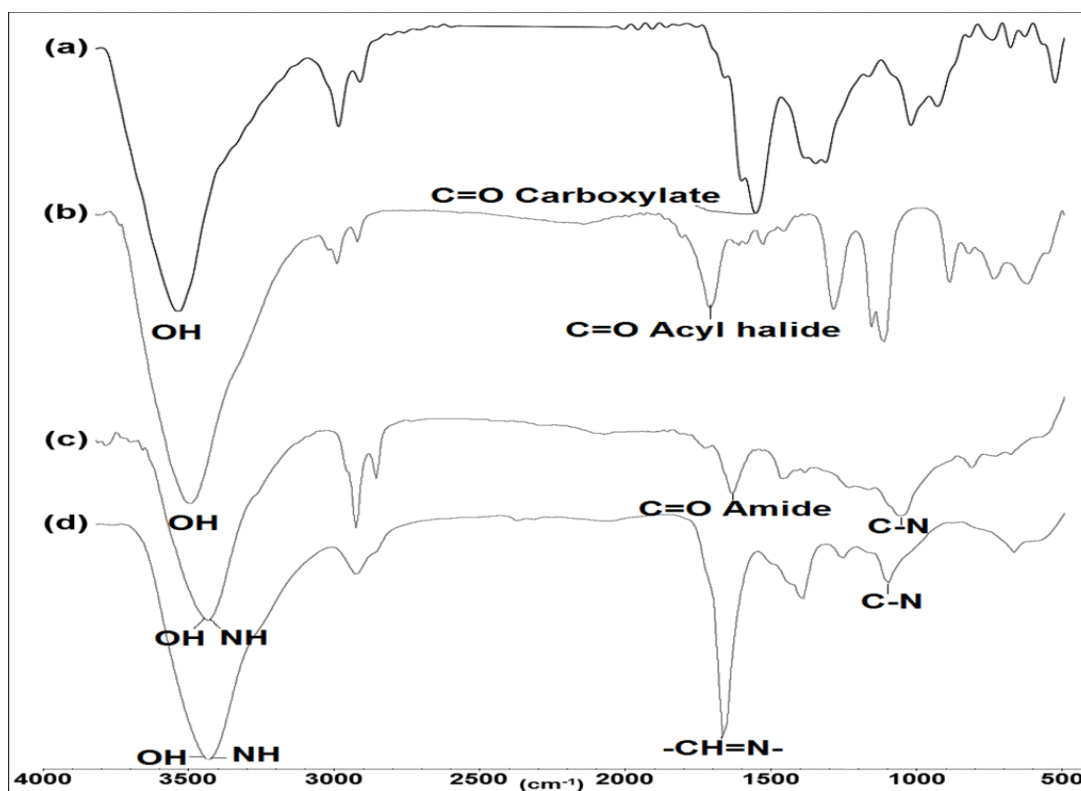
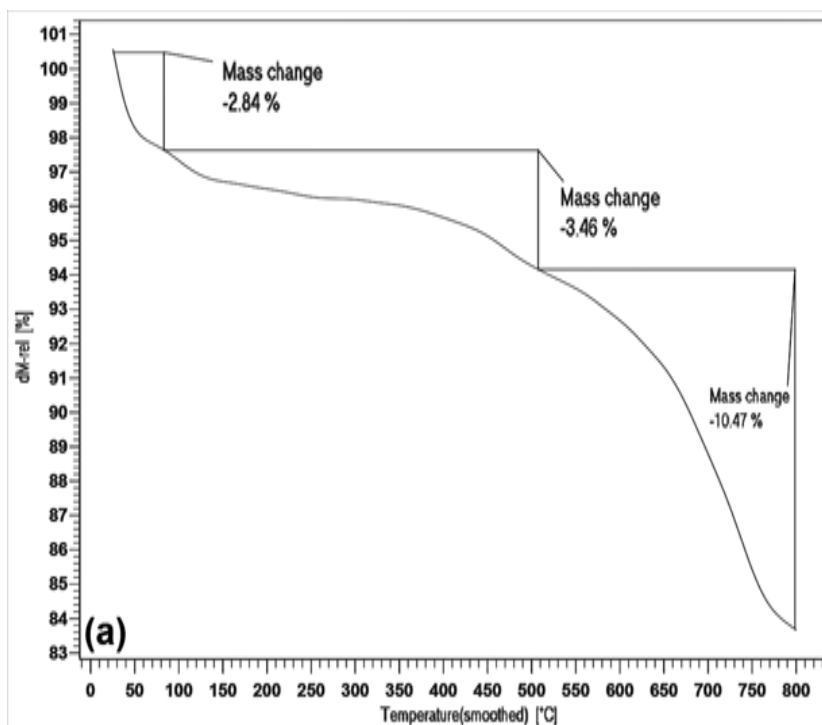


Figure 2. The FT-IR spectra of a) MWCNT; b) chlorinated MWCNT; c) Mel-MWCNT and d) poly Schiff-base

Figure 3. The TGA thermograms of a) MWCNT and b) poly Schiff-bas



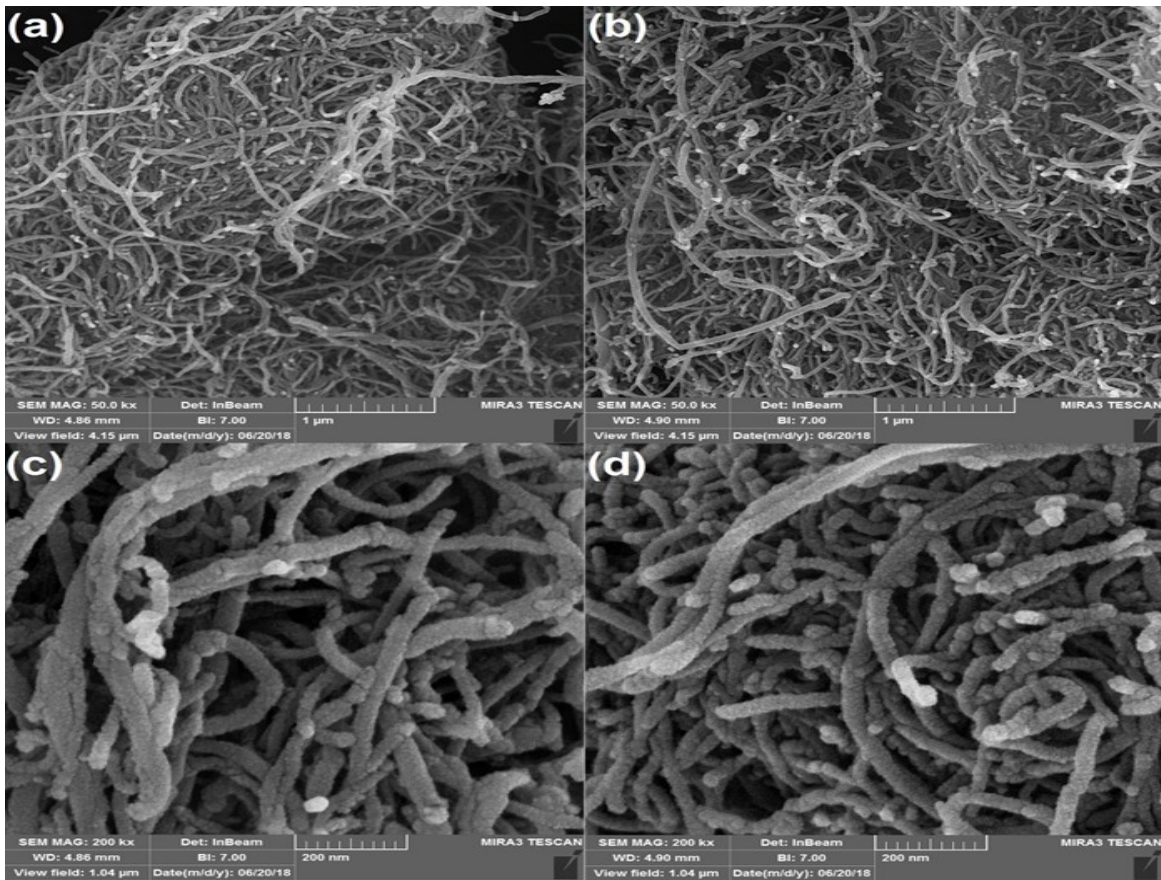
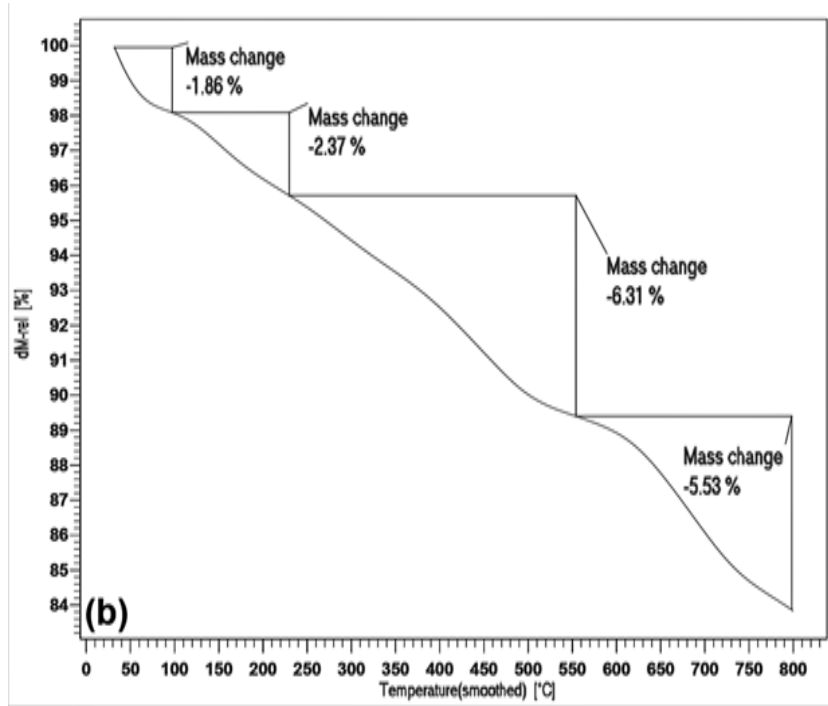


Figure 4. The SEM images of a, c) MWCNT and b, d) poly Schiff-base

MWCNT is small. The tubular structure of the modified sample became relatively thicker and the size of the porosity in the samples slightly reduced. The tubular structure of the adsorbent which is due to the MWCNT backbone is remarkably observable in final product. The porous structure has provided a suitable space to entrap and adsorb the dye molecules. It seems that the pattern of host molecules was replicated in the growth of guest molecules, with a minimal change in morphology.

Adsorption studies

The synthesized poly Schiff-base was examined in dye molecules removal from aqueous solution and CR dye was selected as typical dye. The equilibrium adsorption capacity (q_e , mg/g⁻¹) and the percent removal (R%) were calculated using the follow equations.

$$q_e = (C_0 - C_e) \frac{V}{m} \quad (1)$$

$$R\% = \frac{(C_0 - C_e)}{C_0} \times 100 \quad (2)$$

Where C_0 and C_e (mg/L⁻¹) are the initial and equilibrium concentrations of the dye in mg/L of solution, respectively. V (L) is the volume of the dye solutions and m (g) is the amount of the adsorbent dosage. [Figure 5](#) shows the optimization diagrams of the adsorption parameters. In order to demonstrate the absorption capability of the synthesized adsorbent, its adsorption capacity was compared with similar adsorbents in the Congo red dye adsorption ([Table 1](#)). Comparison of the results showed that the synthesized poly Schiff-base has a good adsorption capacity.

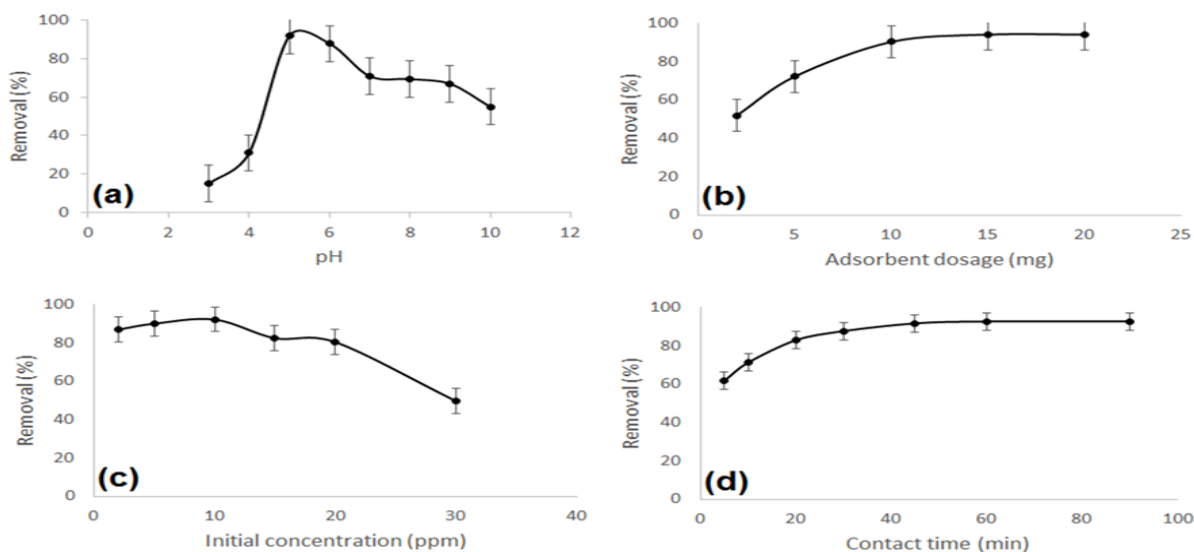


Figure 5. The adsorption diagrams for the optimization of different parameters, a) pH; b) adsorbent amount; c) initial concentration of CR and d) contact time

Table 1. Comparison of adsorption capacities of Congo red on various adsorbents

Adsorbents	Adsorption capacity (mg/g ⁻¹)	Concentration of CR dye(mg/l ⁻¹)	Reference
Hollow Zn-Fe ₂ O ₄ nanospheres	16.1	1-50	37
Activated coir pitch carbon	6.27	20-80	38
Bagasse fly ash	11.88	5-30	38
Activated red mud	7.08	10-90	39
Raw pine cone	19.18	20-50	40
Waste orange peel	22.44	10-50	42
Bruneian peat	10.1	5-400	42
Sodium bentonite	35.84	50-1000	43
Poly Schiff-base based on melamine-modified MWCNT	21.74	2-30	Present study

Effect of pH

The initial pH of the aqueous solution plays an important role in the dye adsorption, affected by the dye chemistry and the sites of the adsorbents. In [Figure 5a](#) which is related to the optimization of the pH, the highest adsorption percentage is obtained at pH=5. The adsorbent active sites are protonated at lower pH values, thus the interaction of the adsorbent with the adsorbate decreased. By increasing the pH value higher than 5, the adsorption percentage was reduced; however, with slower rate rather than the acidic media. In this case, hydroxide ions started to compete with the adsorbent sites to interact with the dye. Hence the capability of the adsorbent decreased gradually. Moreover, the negative charge repulsion between the deprotonated and relatively negative nature of the adsorbent sites in the basic media and the anionic dye is somehow effective.

Effect of adsorbent dosage

Influence of various amount of the initial dosage of adsorbent is demonstrated in [Figure 5b](#). According to this diagram, the adsorption percentage enhanced by increasing the adsorbent dosage up to 15 mg and then it remained at a constant value. It can be simply concluded that the number of active sites increased by enhanced the dosage and it leads to an adsorption percentage increase.

Effect of dye initial concentration

Effect of initial concentration on the removal (%) are shown in [Figure 5c](#). According to this diagram, the adsorption percentage reduced by increasing the initial dye concentration. The results of this experiment revealed that the adsorbent has enough active sites at lower concentrations to

interact with the dye molecules to adsorb 10 ppm of the selected dye concentration, so the adsorption was increased up to 10 ppm. However, due to the occupation of the active sites in 10 ppm, it was observed that by increasing the dye concentration, the adsorption was further decreased. Therefore, the 10 ppm was selected as an optimized point.

Effect of contact time

Optimization of the contact time is also another key parameter in the removal of pollutants. This is due to the fact that, the high contact times do not have remarkable effect on the removal percentage. As seen in [Figure 5d](#), the removal percentage reached to about 90% after 45 min, then no considerable increase was observed. Increasing the contact time lets the adsorbent to interact with the adsorbate more effectively; however, the interaction between the adsorbent and the adsorbate reached to its equilibrium state at higher contact times and no remarkable removal took place. Therefore, in this case, the optimized contact time was selected to be 45 min.

Adsorption isotherms

Adsorption characteristics can be usually described by an adsorption isotherm. The study of the adsorption isotherms is needed to reach to some data in the adsorption mechanism, the surface properties, and the tendency of the adsorbent toward the dye [44–48]. Among many models that can be applied to provide some information about the adsorption mechanism, the Langmuir, Freundlich, and Dubinin-Radushkevich (D-R) adsorption isotherm models are applied in this study to describe the equilibrium between the adsorbed CR molecules on the poly Schiff-base (q_e) and the CR molecules in solution (C_e).

The Langmuir equation is valid for the adsorption processes that take place at homogeneous sites with no transmigration of the adsorbed molecules on the plane of the surface and it is suitable for the monolayer adsorption on the surface of the adsorbent. The Langmuir isotherm is described by the following equation [49]:

$$q_e = \frac{q_m k_1 c_e}{1 + k_1 c_e} \quad (3)$$

The linear form is expressed as:

$$\frac{c_e}{q_e} = \frac{1}{k_1 q_m} + \frac{c_e}{q_m} \quad (4)$$

Where C_e (mg/L^{-1}) is the concentration of the dye solution at the equilibrium state, q_e (mg/g^{-1}) is the amount of the adsorbate adsorbed per unit mass of the adsorbent. q_m (mg/g^{-1}) which is the maximum

adsorption capacity corresponds to the complete monolayer coverage, and K_L (L/mg^{-1}) which is the Langmuir adsorption constant is related to the free energy adsorption. When C_e/q_e is plotted versus C_e , a straight line is obtained, so that the constant values (q_m and K_L) are evaluated from the slope and the y -intercept of the linear plots, respectively. The results are presented in [Figure 6a](#). The amount of the R_L factor can express the essential characteristics of the Langmuir equation. The R_L is defined as follows:

$$R_L = \frac{1}{1+K_L C_0} \quad (5)$$

C_0 (mg/L^{-1}) is the initial dye concentration. The type of isotherm is irreversible ($R_L=0$), favorable ($0<R_L<1$), linear ($R_L=1$), or unfavorable ($R_L>1$) [50]. The R_L values in this study were found to be between 0 and 1 and they showed a favorable adsorption between the CR dye and the adsorbent. The Freundlich isothermal model is suitable for the multilayer adsorption on a heterogeneous adsorbent surface. It is applied to assess the adsorption intensity of the adsorbent to the adsorbate. The Freundlich isotherm model is represented as:

$$q_e = K_f C_e^{\frac{1}{n}} \quad (6)$$

The linear form can be expressed as follows:

$$\ln q_e = \ln K_f + \frac{1}{n} \ln C_e \quad (7)$$

Where K_f is the Freundlich constant (expressing the adsorption capacity), n indicates the intensity of the adsorption. The values of K_f and n are proportional to the y -intercept and the slope of $\ln q_e$ vs. $\ln C_e$ plot, respectively ([Figure 6b](#)). The value of n should be between 1 and 10 and it might change as the heterogeneity of the adsorbent changes. A higher value of K_f indicates a higher capacity of the adsorbent. The (D-R) isotherm which assumes a homogeneous surface is another equation which is applied to estimate the porosity, free energy, and the characteristic of the adsorption [51]. This adsorption model is given by the following equation.

$$q_e = q_{max} e^{-\beta \varepsilon^2} \quad (8)$$

The linear form of the R-D isotherm equation can be defined as:

$$\ln q_e = \ln q_m - \beta \varepsilon^2 \quad (9)$$

Where q_m (mg/g^{-1}) is the amount of the adsorbate on the adsorbent at the equilibrium state, q_m (mg/g^{-1}) is the theoretical saturation capacity, and ε is the Polanyi potential and it can be calculated from the following equation:

$$\varepsilon = RT \ln \left(1 + \frac{1}{C_e} \right) \quad (10)$$

Where R ($8.314 \text{ J/mol}^{-1}/\text{K}^{-1}$) is the gas constant and T (K) is the absolute temperature, β is a constant related to the adsorption energy and gives the mean free energy E (KJ/mol^{-1}) of adsorption per molecule of adsorbate when one mole of it is transferred from the solution to the surface of the sorbent and it can be calculated by using the following equation:

$$E = \frac{1}{\sqrt{2\beta}} \quad (11)$$

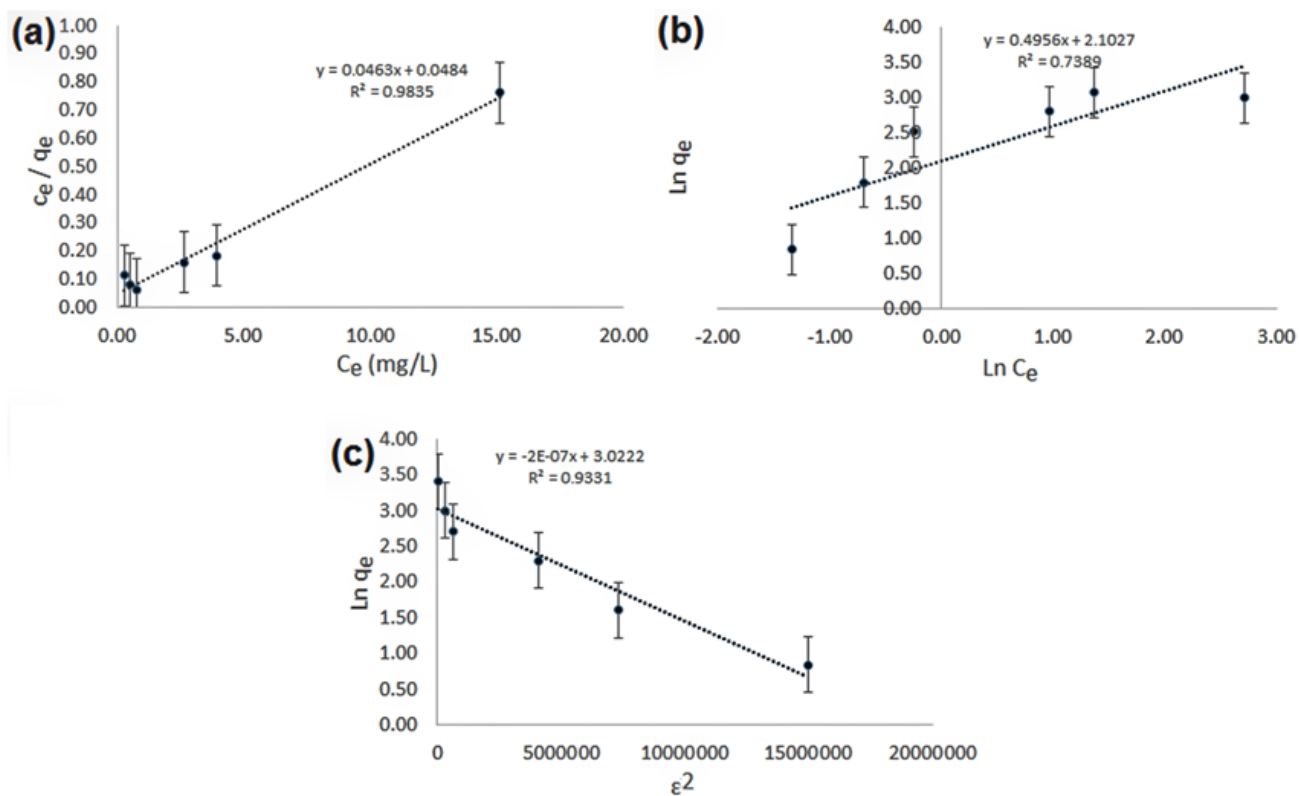


Figure 6. The diagram of adsorption isotherms; a) Langmuir; b) Freundlich and c) Dubinin-Radushkevich (D-R)

It is indicated that the magnitude of this parameter (E) lies between 8 and 16 (KJ/mol^{-1}). It means that the chemical adsorption has taken place and the reaction proceeds physically if it is less than 8

KJ/mol⁻¹. In this study, the E value was calculated to be less than 8 and it indicates that the adsorption of the CR dye occurred physically.

The Langmuir, Freundlich, and D-R parameters for the adsorption of the CR dye onto the synthesized poly Schiff-base are summarized in Table 2. The comparison of these results revealed that the R² value for Langmuir model is closer to unit, indicating the monolayer adsorption of the dye on the adsorbent surface.

Adsorption kinetics

The rate and the mechanism of an adsorption process can be elucidated *via* two kinetic models. These models are the Lagergren pseudo-first-order and the Ho pseudo-second-order equations [9]. The Lagergren kinetic model defines the rate of adsorption proportional to the number of unoccupied sites in the adsorbent surface and is expressed in the following linear equation:

$$\ln(q_e - q_t) = \ln q_e - k_1 t \quad (12)$$

Table 2. The parameter values of adsorption isotherm

Isotherms and linear equations	Parameter	Value
Langmuir $\frac{c_e}{q_e} = \frac{1}{k_1 q_m} + \frac{c_e}{q_m}$	q_m (mg/g ⁻¹)	21.74
	K_L (L/mg ⁻¹)	0.95
	R_L	0.34
	R_2	0.983
Freundlich $\ln q_e = \ln K_f + \frac{1}{n} \ln C_e$	K_f (mg/g ⁻¹)	8.18
	n	2.07
	R_2	0.738
Dubinin–Radushkevich $\ln q_e = \ln q_m - \beta \varepsilon^2$	q_m (mg/g ⁻¹)	20.53
	E (Kj/mol ⁻¹)	1.58
	β (mol ² /kj ⁻²)	2×10^{-7}
	R_2	0.933

Where q_e and q_t (mg/g⁻¹) are the adsorption capacities at the equilibrium state, t is the time (min), and k_1 (min⁻¹) is the pseudo-first-order rate constant for the kinetic model. The values of q_e and k_1 are proportional to the y -intercept and the slope of the $\ln(q_e - q_t)$ is versus t plot, respectively (Figure 7a). The Ho kinetic model assumes that the rate of the adsorption is proportional to the square of the number of the unoccupied sites. This model is represented as:

$$\frac{t}{q_t} = \frac{1}{k_2 q_e^2} + \frac{1}{q_e} t \quad (13)$$

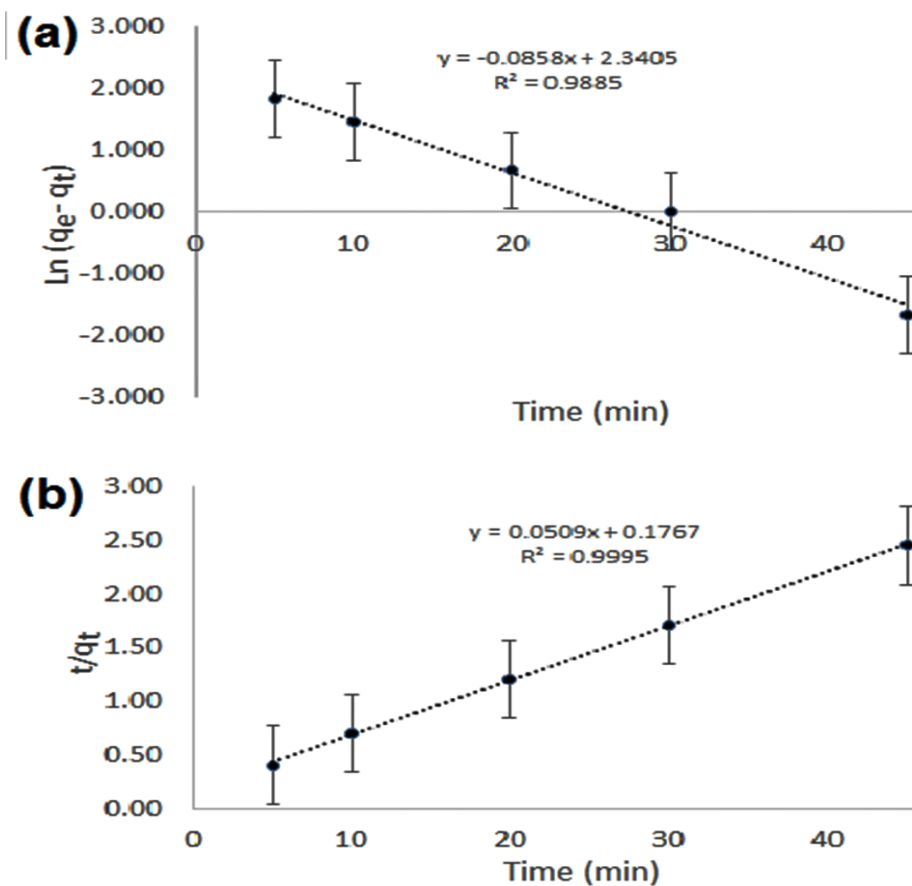


Figure 7. The diagram of adsorption kinetics; a) Lagergren pseudo-first-order and b) Ho pseudo-second-order

Table 3. The parameter values of adsorption kinetics

Kinetic models and parameters	Value
Pseudo-first-order model	
$q_{e,exp}$ (mg/g ⁻¹)	18.52
$q_{e,cal}$ (mg/g ⁻¹)	10.38
k_1 (min ⁻¹)	0.085
R^2	0.988
Pseudo-second-order model	
$q_{e,exp}$ (mg/g ⁻¹)	18.52
$q_{e,cal}$ (mg/g ⁻¹)	19.26
k_2 (g/mg ⁻¹ /min ⁻¹)	0.017
R^2	0.999

Where k_2 ($\text{g}/\text{mg}^{-1}/\text{min}^{-1}$) is the pseudo-second-order adsorption kinetic parameter, k_2 and q_e can be obtained from the slope and y-intercept of (t/q_t) versus t plot (Figure 7b). The experimental values of two kinetic models are calculated and presented in Table 3. The calculated equilibrium adsorption capacities ($q_{e,\text{cal}}$) and the experimental ($q_{e,\text{exp}}$) values from the pseudo-second-order kinetic model are very close to each other respected to the pseudo-first-order kinetics. On the other hand, the R^2 value for pseudo-second-order kinetic model is found to be higher than that of the pseudo-first-order kinetics. Therefore, the pseudo-second-order kinetic model with an excellent correlation (R^2) coefficient and $q_{e,\text{cal}}$ which is close to $q_{e,\text{exp}}$ is more applicable to describe the adsorption process of the CR dyes on the synthesized poly Schiff-base.

Conclusions

In this study, the MWCNT-based poly Schiff-base was synthesized to be utilized as an efficient adsorbent for the removal of the dye from the aqueous solutions. In the first step, carboxylated MWCNT was chlorinated to generate highly active acyl halides to react with excess amount of melamine. Free NH_2 pendant groups were then reacted with 3-pyridinecarboxaldehyde to prepare the final poly Schiff-base. In the final step, the adsorption study was carried out to investigate and optimize the effective parameters. Moreover, the adsorption isotherms and kinetics were also studied to show the mechanism of the adsorption. According to the results, the prepared adsorbent can be a good candidate for the removal of the dyes with similar structure to Congo red dye as a pollutant from aqueous solutions. Also the adsorption isotherms studies indicated that, the adsorption of the dye occurred physically. Moreover, the adsorption kinetics studies revealed that, the pseudo-second-order kinetic model was more applicable to describe the adsorption process of the CR dyes on the synthesized poly Schiff-base.

Acknowledgements

The authors would like to acknowledge the financial and spiritual supports from the Urmia University, Iran.

Disclosure Statement

No potential conflict of interest was reported by the authors.

References

- [1]. Gupta V.K., Ali I., Saini V.K. *Water Res.*, 2007, **41**:3307
- [2]. Gupta V.K., Srivastava S.K., Mohan D., Sharma S. *Waste Manag.*, 1998, **17**:517

- [3]. Gupta V.K., Jain R., Varshney S., Saini V.K. *J. Coll. Interf. Sci.*, 2007, **307**:326
- [4]. Gupta V.K., Mohan D., Suhas, Singh K.P. *Ind. Eng. Chem. Res.*, 2006, **45**:1113
- [5]. Van der Zee F.P., Villaverde S. *Water Res.*, 2005, **39**:1425
- [6]. Crini G. *Bioresource Technol.*, 2006, **97**:1061
- [7]. Taghizadeh F., Ghaedi M., Kamali K., Sharifpour E., Sahraie R., Purkait M.K. *Powder Technol.*, 2013, **245**:217
- [8]. Sheibani M., Ghaedi M., Marahel F., Ansari A. *Desalin. Water Treat.*, 2015, **53**:844
- [9]. Ahmadi K., Ghaedi M., Ansari A. *Acta A: Mol. Biomol. Spectros.*, 2015, **136**:1441
- [10]. Ali I., Asim M., Khan T.A. *J. Environ. Manage.*, 2012, **113**:170
- [11]. Ghaedi M., Kokhdan S.N. *Desalin. Water Treat.*, 2012, **49**:317
- [12]. An J.S., Back Y.J., Kim K.C., Cha R., Jeong T.Y., Chung H.K. *Environ. Technol.*, 2014, **35**:1668
- [13]. Li C., Zhuang Z., Huang F., Wu Z., Hong Y., Lin Z. *ACS Appl. Mater. Interfaces*, 2013, **5**:9719
- [14]. Du X., Zhang H., Hao X., Guan G., Abudula A. *ACS Appl. Mater. Interfaces*, 2014, **6**:9543
- [15]. Fu L., Shuang C., Liu F., Li A., Li Y., Zhou Y., Song H. *J. Hazard. Mater.*, 2014, **272**:102
- [16]. Deng S.J., Wang R., Xu H.J., Jiang X.S., Yin J. *J. Mater. Chem.*, 2012, **22**:10055
- [17]. Deng S.J., Xu H.J., Jiang X.S., Yin J. *Macromolecules*, 2013, **46**:2399
- [18]. Wei X.Z., Kong X., Wang S.X., Xiang H., Wang J.D., Chen J.Y. *Ind. Eng. Chem. Res.*, 2013, **52**:17583
- [19]. Liu W., Wu Z.L., Wang Y.J., Zhao Y.L., Liu W.C., Yu Y. *Ind. Eng. Chem. Res.*, 2013, **52**:13761
- [20]. Li B., Dong Y.C., Zou C., Xu Y.M. *Ind. Eng. Chem. Res.*, 2014, **53**:4199
- [21]. Yadav A., Mukherji S., Garg A. *Ind. Eng. Chem. Res.*, 2013, **52**:10063
- [22]. Rodrigues C.S.D., Madeira L.M., Boaventura R.A.R. *Ind. Eng. Chem. Res.*, 2014, **53**:2412
- [23]. Tastan B.E., Karatay S.E., Donmez G. *Water Sci. Technol.*, 2012, **66**:2177
- [24]. Liu F., Chung S., Oh G., Seo T.S. *ACS Appl. Mater. Interfaces*, 2012, **4**:922
- [25]. Dou X., Li P., Zhang D., Feng C.L. *Soft Matter.*, 2012, **8**:3231
- [26]. Zhu X., Liu Y., Zhou C., Zhang S., Chen J. *ACS Sustainable Chem. Eng.*, 2014, **2**:969
- [27]. Liu L., Gao Z.Y., Su X.P., Chen X., Jiang L., Yao J.M. *ACS Sustainable Chem. Eng.*, 2015, **3**:432
- [28]. Cifuentes A.R., Avila K., García J.C., Daza C.E. *Ind. Eng. Chem. Res.*, 2013, **52**:16197
- [29]. Zhang C.M., Song W., Sun G.H., Xie L.J., Wan L., Wang J.L., Li K.X. *Ind. Eng. Chem. Res.*, 2014, **53**:4271
- [30]. Lakouraj M.M., Mojerlou F., Zare E.N. *Carbohydr. Polym.*, 2014, **106**:34
- [31]. Zare E.N., Lakouraj M.M. *Iran. Polym. J.*, 2014, **23**:257
- [32]. Zare E.N., Motahari A., Sillanpaa M. *Environ. Res.*, 2018, **162**:173
- [33]. Zare K., Gupta V.K., Moradi O., Makhlof A.S.H., Sillanpaa M., Nadagouda M.N., Sadegh H., Shahryari-ghoshekandi R., Pal A., Wang Z.J., Tyagi I., Kazemi M. *J. Nanostruct. Chem.*, 2015, **5**:227

- [34]. Gao H., Zhao S., Cheng X., Wang X., Zheng L. *Chem. Eng. J.*, 2013, **223**:84
- [35]. Ihsanullah A.A., Al-Amer A.M., Laoui T., Almarri M., Nasser M., Khraisheh M., Atieh M.A. *Sep. Purif. Technol.*, 2016, **157**:141
- [36]. Wang L.X., Li J.C., Wang Y.Q., Zhao L.J., Jiang Q. *Chem. Eng. J.*, 2012, **181**:72
- [37]. Namasivayam C., Kavitha D. *Dyes Pigments*, 2002, **54**:47
- [38]. Mall I.D., Srivastava V.C., Agarwal N.K., Mishra I.M. *Chemosphere*, 2005, **61**:492
- [39]. Tor A., Cengeloglu Y. *J. Hazard. Mater.*, 2006, **138**:409
- [40]. Dawood S., Sen T.K. *Water Res.*, 2012, **46**:1933
- [41]. Namasivayam C., Muniasamy N., Gayatri K., Rani M., Ranganathan K. *Bioresour. Technol.*, 1996, **57**:37
- [42]. Zehra T., Priyantha N., Lim L.B.L., Iqbal E. *Desalin. Water Treat.*, 2014, **54**:2592
- [43]. Vimonses V., Lei S., Jin Bo., Chow C.W.K., Saint C. *Chem. Eng. J.*, 2009, **148**:354
- [44]. Venkateswarlu S., Yoon M. *ACS Appl. Mater. Interfaces*, 2015, **7**:25362
- [45]. Ghaedi M., Zamani Amirabad S., Marahel F., Nasiri Kokhdan S., Sahraei R., Nosrati M., Daneshfar A. *Spectrochim. Acta Part A.*, 2011, **83**:46
- [46]. Langmuir I. *J. Am. Chem. Soc.*, 1916, **38**:2221
- [47]. Abdelwahab O. *Desalination*, 2008, **222**:357
- [48]. Ng C., Losso J.N., Marshall W.E., Rao R.M. *Bioresour. Technol.*, 2002, **85**:131
- [49]. Ai L., Zhang C., Chen Z. *J. Hazard. Mater.*, 2011, **192**:1515
- [50]. Hao Y.M., Man C., Hu Z.B. *J. Hazard. Mater.*, 2010, **184**:392
- [51]. Hall K.R., Eagleton L.C., Acrivos A., Vermeulen T. *Ind. Eng. Chem. Fundam.*, 1966, **5**:212

How to cite this manuscript: Somayeh Farajzadeh, Peyman Najafi Moghadam*, Jabbar Khalafy. Removal of colored pollutants from aqueous solutions with a poly Schiff-base based on melamine-modified MWCNT. *Asian Journal of Green Chemistry*, 4(4) 2020, 397-415. DOI: [10.22034/ajgc.2020.100567](https://doi.org/10.22034/ajgc.2020.100567)